LIF Measurement of Interacting Gas Jet Flow with Plane Wall

A. Yanagi[a], S. Kurihara[a], S. Yamazaki[a], M. Ota[b], and K. Maeno[b]

[a]Graduate Student, [b]Graduate School of Engineering, Chiba University
1-33 Yayoi, Inage, Chiba, #263-8522, JAPAN

Abstract. Discharging rarefied gas jets in low-pressure conditions are interesting and important phenomena from an engineering point of view. For example they relate to the attitude control of the space satellite, or the semiconductor technology. The jets, however, deform to the complicated shapes by interacting with solid walls. In this paper we have performed the experiments the flow visualization as a first step by applying the LIF (Laser Induced Fluorescence) method on the jet-wall interaction. Jet is spouting out from a φ1.0mm circular hole into the low pressure air chamber, impinging on a flat plate. The LIF visualization of interacting rarefied gas jet is carried out by using the iodine (I_2) tracer and argon ion laser.

Keywords: LIF method, Iodine, Gas jet, Jet-wall interaction, Visualization

INTRODUCTION

Discharging rarefied gas jet flow interacts occasionally with such neighboring solid structure as plane wall and equipments, which produces interference problem with structure in space. Recently gas jet is also used to improve the processing accuracy of semiconductor surface and so on. For that purpose, the distributions of rarefied gas jet flow parameters should be investigated to obtain more precise flow information such as velocity and density distributions of the interacting field. The visualization of axi-symmetric nozzle free jet flow and many numerical simulations have been conducted since 1980s [1]. In this study, we have performed the experiments of the interacting jet flow visualization, as a fundamental research, by applying the LIF (Laser Induced Fluorescence) measurement on low-pressure jet, which is discharging out from axi-symmetric nozzle with a flat plate, to the vacuum chamber [2]. The LIF measurement is the method to visualize the flow field by utilizing the fluorescence of phosphor [3]. The LIF measurement has high sensitivity, and is suitable for the measurement of the field where the temperature and the density change are significant. In addition, the method is possible to measure the flow field without causing turbulent flow, because LIF measurement is noncontact method at the arbitrary section of flow field by changing the laser irradiation position. However, it is not easy to obtain the physical values of the flow parameters quantitatively because the fluorescence intensity depends both on the density and the thermodynamic state of the iodine, and so on [4-7]. Therefore, we assumed that measured LIF intensity is mainly due to density field and attempted to obtain density distribution of the flow field from the fluorescence image.

EXPERIMENTAL APPARATUS AND VISUALIZATION

The experimental apparatus of LIF experiment is shown in Fig.1. The argon gas is mixed with iodine (I_2) as tracer through thin tube and spouts out from the nozzle into vacuum chamber as discharging gas jets. The gas jet is irradiated with a sheet-shaped argon ion laser beam, which is shaped into sheet using the lens, collimator lens and cylindrical lenses, and the jet generates the longer-wavelength fluorescence compared with the wavelength of argon ion laser (AUTEX, H800AMaFF7, max 1.1W). The argon ion laser wavelengths are 457.9nm-514.5nm, where the power rate of the wavelengths of 488.0nm and 514.5nm accounts for 40-45%. As a result, the iodine molecules in the jets are excited by argon ion laser, and they generated the fluorescence [8]. The LIF images are taken with a CCD high

sensitivity camera (HAMAMATSU, ORCA-ER-12AG, C4742-80), and the measured stagnation pressure and background pressure signals are also sent to the oscilloscope. In addition the quantity of gas flow is controlled by a regulator, which maintains a steady state (the background pressure P_{cb} is about 0.6kPa and the stagnation pressure P_{st} is about 8.0kPa) in low pressure test chamber. The bandpass filter that passes only specific wavelength range (central wavelength is 585nm and half-value width is 10nm) is fixed on the CCD camera. The CCD camera is set perpendicular to the interacting jet. Thus argon ion laser sheet is irradiated to out the flow field and CCD high sensitivity camera is used to have an image of the flow. The image data are sent to a personal computer, and are processed to obtain the fluorescence intensity distribution from these images.

The experimental model with coordinate system is shown in Fig.2. As well, the original point of *x*-*y*-*z* coordinate system is defined as the center of nozzle (φ1.0mm circular hole). The images of the jet in the *x*-*z* plane are obtained by irradiating sheet-shaped laser parallel to the jet and the *y*-*z* plane are obtained by irradiating sheet-shaped laser vertically to the jet. In this way, the visualization images of gas jet *x*-*z* and *y*-*z* plane are obtained by changing the position of sheet-shaped argon ion laser beam. Furthermore, the schematic of the model layout and cross section of nozzle (diameter of nozzle is 1mm) is shown in Fig.3. The angle between direction of gas jet and plane wall is defined as θ. In this paper we deal with visualization results of θ = 30, 45, and 60°. Additionally, the analysis range bounded by the square (Fig.3 (b)) is discussed in the section of "RESULTS AND DISCUSSION".

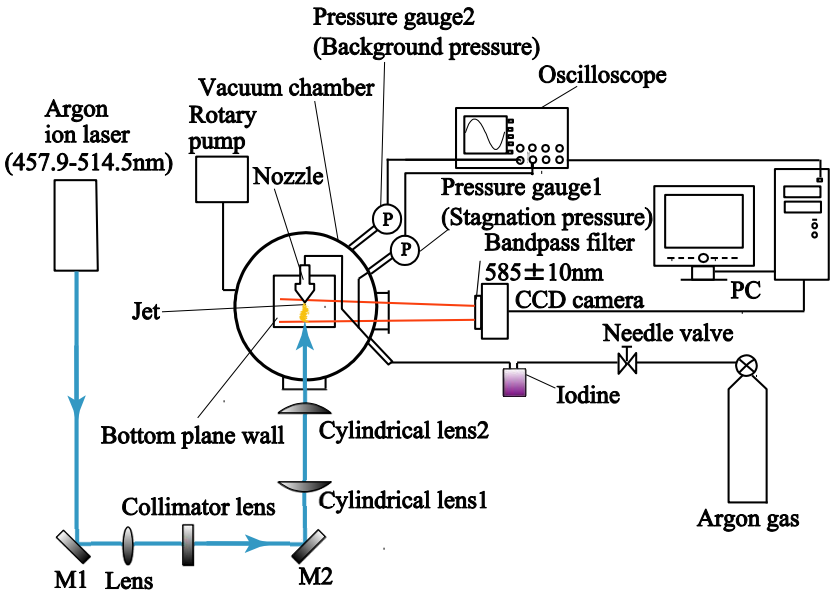

FIGURE 1. Experimental apparatus

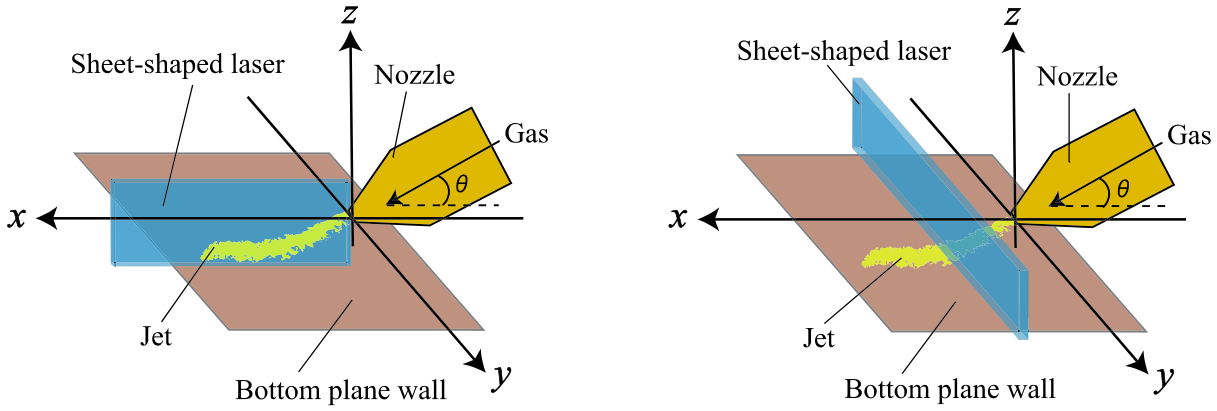

(a) *x*-*z* plane (b) *y*-*z* plane

FIGURE 2. The experimental model with coordinate system

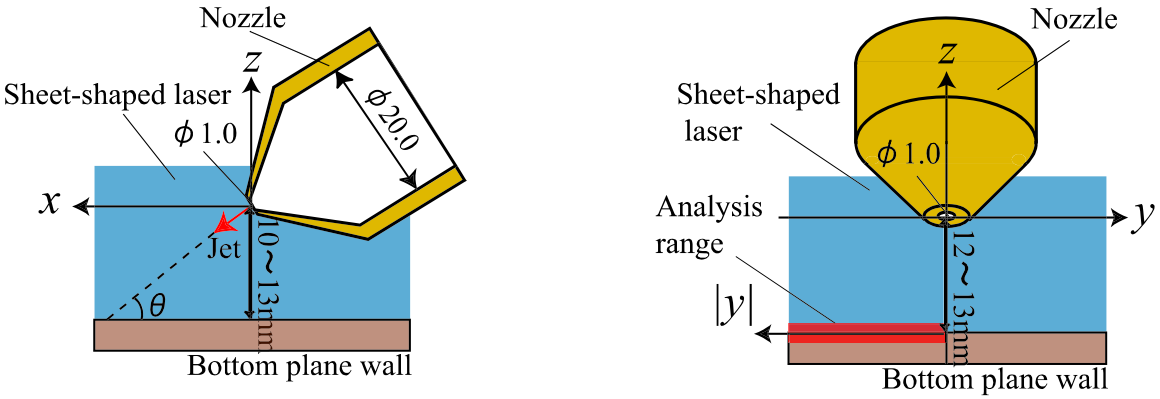

(a) *x*-*z* plane (b) *y*-*z* plane

FIGURE 3. The schematic of the model layout and cross section of nozzle

RESULTS AND DISCUSSION

The experimental results taken by CCD camera are shown in Fig.4 and Fig.5. Figure 4 shows the normalized intensity image of *x*-*z* plane at y = 0mm interacting rarefied gas flow with a flat plate at an angle of 30, 45, and 60°. Also, the normalized intensity images of interacting rarefied gas flow, *y*-*z* plane of θ = 30° at *x* = 20, 22mm (vicinity of the jet impinging point) and *x* = 26, 30mm (far from the impinging point) are shown in Fig.5 (a). In turn, the images of gas flow, *y*-*z* plane of θ = 45° at *x* = 10, 12mm and *x* = 16, 20mm are shown in Fig.5 (b), and *y*-*z* plane of θ = 60° at *x* = 6, 8mm and *x* = 12, 16mm are shown in Fig.5(c). In these images measured fluorescence intensity (*I*) is normalized by I_0, fluorescence intensity average value of overall image of time before starting gas flow. Each of normalized intensity value (I/I_0) is represented by a different color, (in case of I/I_0 = 1.0~1.1, the field is brown, I/I_0 = 1.1~1.2 is red, I/I_0 = 1.2~1.3 is orange, I/I_0 = 1.3~1.4 is yellow, and over I/I_0 = 1.4 it is white). The color bar is also shown in Fig.4. In this way, the patterns of the flow field and characteristics of gas jet are figured out. As a result, the central part of gas jet spouted out from nozzle flows straight, and collides with plane wall and after the impingement the gas jet flows along the plane wall. In addition, after the impinging, gas jet spreads over the area on the *y* axis. Also the gas jet soars high just after impinging in the case of θ = 60°.

In this paper we regard the behavior of interacting rarefied gas flow as left-right symmetry, and we analyzed the behavior of gas flow at the analysis range bounded by the thin square zone(Fig.3 (b)), which locates on the surface of plane wall. We measured the boundary position of each normalized intensity (I/I_0 = 1.1, 1.2, 1.3, and 1.4) near the surface of plane wall. To decide the normalized intensity of the pixel zone (4pixels) in the measured flow field image, we had the following procedure. First, a cell in the analysis range of the normalized image is picked up. Besides in light of variation of normalized fluorescence intensity value, we took into account the 9cells which are a measuring cell and surrounding 8cells. The number of cells beyond the level, for example 1.1, 1.2, 1.3, 1.4, is defined as N. Then the measuring point is defined as “the level” in case of N＜5. On the other hand, the measuring point is defined as “other” in case of N≧5. In this way, we measured the boundary location of normalized fluorescence intensity on the surface of plane wall of each 1.1, 1.2, 1.3 and 1.4zone. These results are shown in Fig.6 (a, b, c). The horizontal axis is *y*-coordinate, and vertical axis is *x*-coordinate. In addition, straight line in these figures marks the impinging position of gas jet at plane wall.

As a result in these figures, normalized fluorescence intensity of the central part is highest, and decreases with distance from central part with either experiment. Then as regards the boundary position of I/I_0 = 1.4, in the case of θ = 30° at *x* = 22mm and θ = 45° at *x* = 12mm, the boundary position is located at about 6~7 times width (|*y*| = 3.2~3.6mm) for nozzle diameter (φ1.0mm), while the results of θ = 60° at *x* = 8mm, the boundary position is located at about 24 times width (|*y*| = 12.1mm). In turn, in the case of θ = 30° at *x* = 30mm and θ = 45° at *x* = 20mm the boundary position is located at about 7~10 times width (|*y*| = 3.7~4.9mm) for nozzle diameter, while θ = 60° *x* = 16mm the boundary position is located at about 6 times width (|*y*| = 2.8mm).

thirdly, as regards the boundary position of I/I_0 = 1.2, in the case of θ = 30° at *x* = 30mm, the boundary position is

located at about 21 times width ($|y|$ = 10.4mm) for nozzle diameter, and for θ = 45° at x = 20mm the boundary position is located at about 60 times wider point ($|y|$ = 30.0mm) for the nozzle diameter, and for θ = 60° at x = 16mm, the boundary position is located at about 52 times wider point ($|y|$ = 26.2mm) for the nozzle diameter. That is to say, in the case of θ = 30 and 45°, similar behavior of gas jet is observed. Gas jet flows along the plane wall without strong reflection after the impingement. Then the gas jet spreads over the area on the y axis with increasing the distance from the jet impinging position. On the other hand, in the case of θ = 60°, different behavior is observed. The gas jet does not spread over the area along the x axis at ever far from the jet impinging position. Instead of it, the gas jet spreads over wide area on the y axis and soars high just after the jet impinging position. This phenomenon is considered by the effects created by soaring of gas jet. Therefore, the larger the angle, the reaching area of gas jet near the surface of plane wall is wider in the vicinity of the jet impinging position.

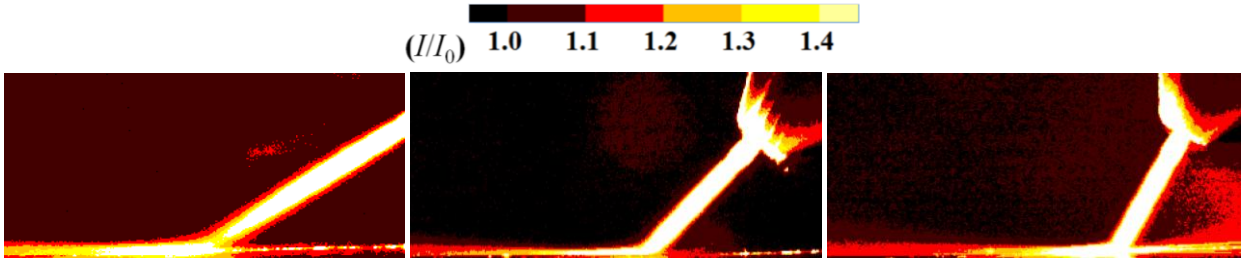

(a) θ = 30°, y = 0mm (b) θ = 45°, y = 0mm (c) θ = 60°, y = 0mm

FIGURE 4. Normalized intensity images of x-z plane interacting rarefied gas flow

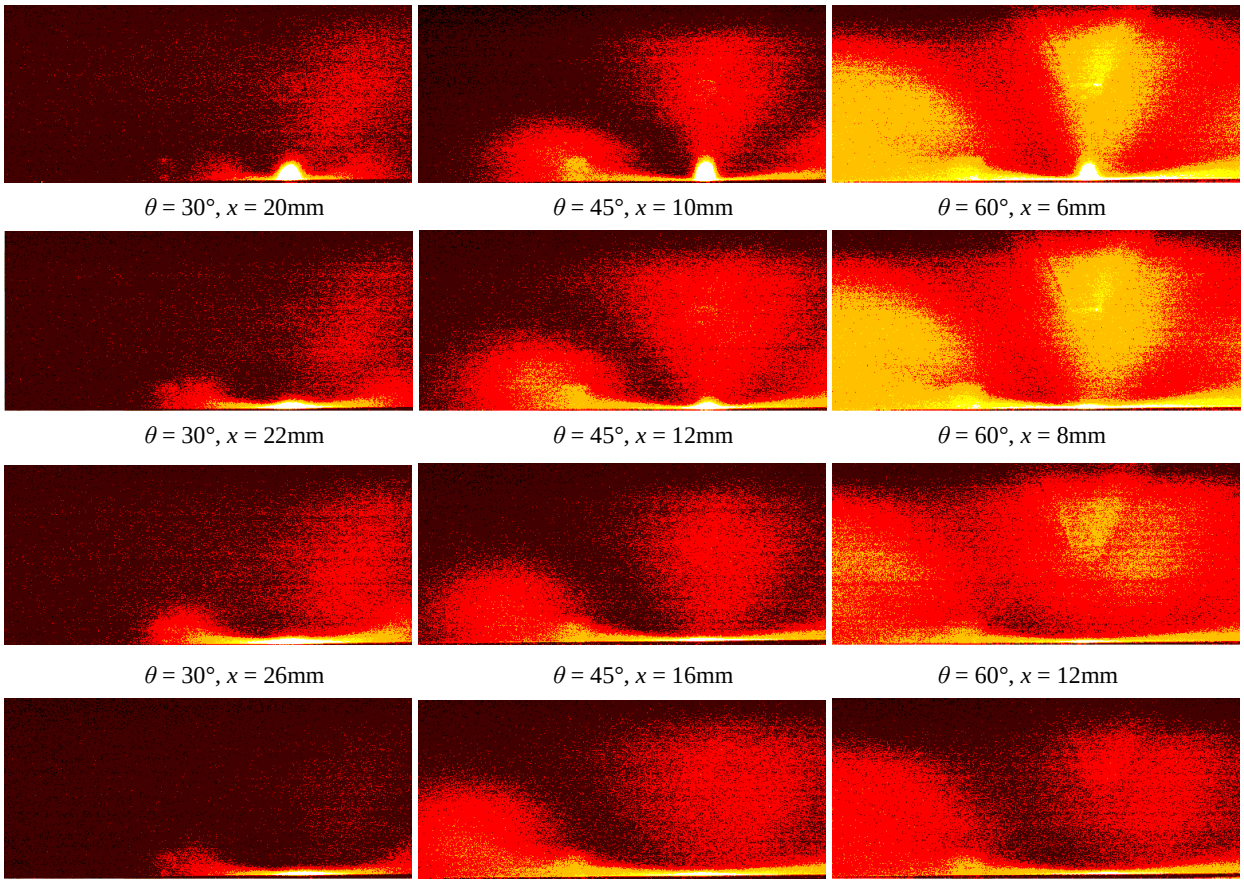

θ = 30°, x = 20mm θ = 45°, x = 10mm θ = 60°, x = 6mm

θ = 30°, x = 22mm θ = 45°, x = 12mm θ = 60°, x = 8mm

θ = 30°, x = 26mm θ = 45°, x = 16mm θ = 60°, x = 12mm

(a) θ = 30°, x = 30mm (b) θ = 45°, x = 20mm (c) θ = 60°, x = 16mm

FIGURE 5. Normalized intensity images of y-z plane interacting rarefied gas flow

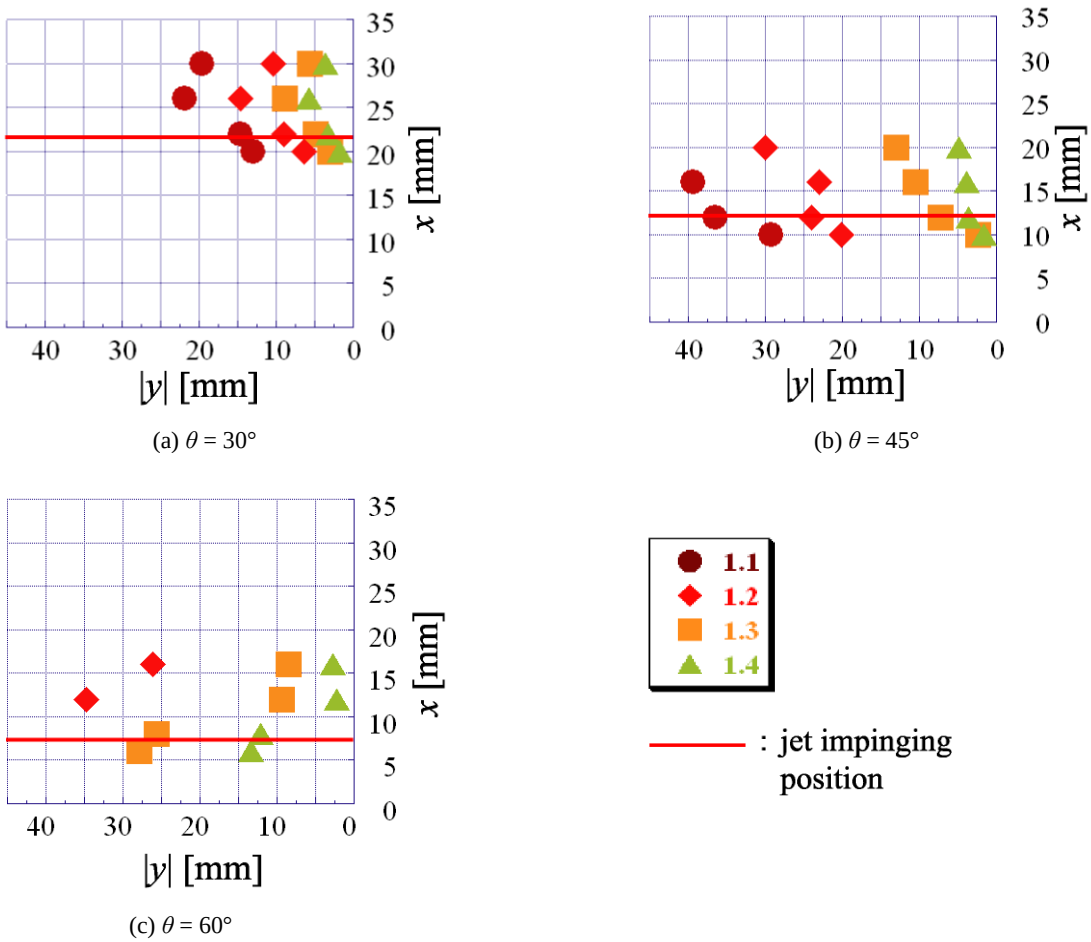

(a) $\theta = 30°$

(b) $\theta = 45°$

(c) $\theta = 60°$

FIGURE 6. Boundary position of normalized intensity near the surface of plane wall

CONCLUSION

In this study we have performed the experiments of the interacting gas jet flow visualization by applying the iodine LIF measurement under low-pressure condition using CCD high sensitivity camera. The normalized intensity images in *y-z* plane of interacting rarefied gas flow with a plane wall at different angle (30, 45, and 60°) are obtained. The results show that the behavior of interacting rarefied gas flow with a plane wall depends heavily on the impinging jet angle. From the normalized intensity image analysis, the patterns of the flow field and characteristics of interacting gas jet are figured out.

Future research activity will be devoted to examine the detailed effects of angle between plane wall and the direction of gas jet on behavior of interacting rarefied gas flow with a plane wall, and of the distance between the plane wall and the nozzle and physical characteristics of plane wall. Furthermore the corrosion of iodine is so strong that, if possible, we would like to make an attempt to visualize rarefied gas flow using other LIF method as acetone [9, 10].

REFERENCES

1. K. Tesima : Visualization of supersonic jets by a laser induced fluorescence method (in Japanese), The Review of Laser Engineering, 12 (1984), 3-10.
2. S. Tsuda : Flow visualization and structural analysis of free jets by LIF method (in Japanese), *NAL TM-741* (1999), 1-9.

3. K. H. An, and I. S. Lee: Temperature measurement around the room air conditioner using the LIF technique, JSME International Journal, Series B, 43 (2000), 622-627.
4. George Kychakoff, Robert D. Howe, Ronald K. Hanson, and James C. McDaniel : Quantitative visualization of combustion species in a place, Applied Optics, 21(18), (1982), 3225-3227.
5. I. van Cruyningen, A. Lozano, and R. K. Hanson : Quantitative imaging of concentration by planar laser-induced fluorescence, Experiments in Fluids 10 (1990), 41-49.
6. P. H. Paul, I. van Cruyningen, R. K. Hanson and G. Kychakoff : High resolution digital flowfield imaging of jets, Experiments in Fluids 9 (1990), 241-251.
7. F. Lemonie, Y. Antoine, M. Wolff, and M. Lebouche : Simultaneous temperature and 2D velocity measurements in a turbulent heated jet using combined laser induced fluorescence and LDA, Experiments in Fluids 26 (1999), 315-323.
8. B. Hiller and R. K. Hanson : Properties of the iodine molecule relevant to laser-induced fluorescence experiments in gas flows, Experiments in Fluids 10 (1990), 1-11.
9. M. C. Thurber, R. K. Hanson : Simultaneous imaging of temperature and mole fraction using acetone planar laser-induced fluorescence, Experiments in Fluids 30 (2001), 93-101.
10. A. Lozano, B. Yip and R. K. Hanson : Acetone: a tracer for concentration measurements in gaseous flows by planar laser-induced fluorescence, Experiments in Fluids 13 (1992), 369-376.